

Review Article

Temporal Considerations for Stimulating Spiral Ganglion Neurons with Cochlear Implants

JASON BOULET,¹ MARK WHITE,² AND IAN C. BRUCE³

¹*McMaster Integrative Neuroscience Discovery and Study, McMaster University, 1280 Main Street West, Hamilton, ON, Canada L8S 4K1*

²*Cary, NC, USA*

³*Department of Electrical and Computer Engineering, McMaster University, 1280 Main Street West, Hamilton, ON, Canada L8S 4K1*

Received: 16 April 2015; Accepted: 14 September 2015; Online publication: 26 October 2015

ABSTRACT

A wealth of knowledge about different types of neural responses to electrical stimulation has been developed over the past 100 years. However, the exact forms of neural response properties can vary across different types of neurons. In this review, we survey four stimulus-response phenomena that in recent years are thought to be relevant for cochlear implant stimulation of spiral ganglion neurons (SGNs): refractoriness, facilitation, accommodation, and spike rate adaptation. Of these four, refractoriness is the most widely known, and many perceptual and physiological studies interpret their data in terms of refractoriness without incorporating facilitation, accommodation, or spike rate adaptation. In reality, several or all of these behaviors are likely involved in shaping neural responses, particularly at higher stimulation rates. A better understanding of the individual and combined effects of these phenomena could assist in developing improved cochlear implant stimulation strategies. We review the published physiological data for electrical stimulation of SGNs that explores these four different phenomena, as well as some of the recent studies that might reveal the biophysical bases of these stimulus-response phenomena.

Keywords: auditory nerve fiber, ion channel, refractoriness, facilitation, accommodation, spike rate adaptation

INTRODUCTION

Cochlear implants (CIs) are prosthetic devices that attempt to provide a coherent auditory perception to individuals with severe to profound deafness. The CI's electrode array resides in the cochlea where it communicates with the user's auditory system by sending out a series of short electrical pulses to type I spiral ganglion neurons (SGNs). Figure 1A shows an electrode array placed in the scala tympani of the cochlea (drawn as a wireframe) where the colors (blue, green, yellow, red) represent the subpopulations of SGNs targeted by the corresponding stimulating electrodes. Note that the term spiral ganglion neuron or cell sometimes refers just to the cell body or soma. It is also common to refer to the bipolar peripheral and central neurites of the SGN as auditory nerve fibers (ANFs). Unless otherwise specified, the term SGN used in this paper will refer to the whole spiral ganglion neuron. Importantly, SGN firing patterns are different in multiple aspects when comparing acoustic and electrical stimulation (Hartmann et al. 1984; Javel and Viemeister 2000). Under acoustic stimulation, SGNs have a greater dynamic range, a more variable firing rate, and they undergo weaker phase locking. In the healthy ear, SGNs act as the bridge connecting the peripheral to

Correspondence to: Jason Boulet · McMaster Integrative Neuroscience Discovery and Study · McMaster University · 1280 Main Street West, Hamilton, ON, Canada L8S 4K1. email: jason.boulet@gmail.com

the central nervous system. More specifically, they receive synaptic input from inner hair cells (IHCs) and output to a variety of cell types in the cochlear nucleus. As such, these neurons act as crucial contributors to the auditory system since they serve as the first layer of auditory neurons encoding afferent spiking information. Inner hair cells release synaptic vesicle packets in a probabilistic nature (Glowatzki and Fuchs 2002; Heil et al. 2007; Safieddine et al. 2012) which could be responsible for the high variability of SGN firing rates in acoustic stimulation. In contrast, when electrically stimulated with a cochlear implant, SGNs are directly excited by voltage-gated ion channel activity.

With the aim of improving speech perception in individuals with cochlear implants, an early approach was to ascertain whether or not increasing the stimulation pulse rate could improve the information transfer to the SGN (e.g., Wilson et al. 1988). Figure 1 shows that due to a current spread in the cochlea and by using a single-channel rate of 900 pulses/s, an SGN can be exposed to an effective rate of 7200 pulses/s when stimulation is delivered by eight electrodes. Some studies have shown that subjects prefer high single-channel stimulation rates in the range of 1700

to 4000 pulses/s (Nie et al. 2006; Verschuur 2005; Kiefer et al. 2000; Loizou et al. 2000), others demonstrated no benefit (Friesen et al. 2005; Plant et al. 2002; Weber et al. 2007; Holden et al. 2002; Plant et al. 2007; Arora et al. 2009), while other research indicates that low to moderate stimulation rates, i.e., 250 to 500 pulses/s, work best (Balkany et al. 2007; Vandali et al. 2000). Significantly, most of these studies report large variance between the performance of individuals as a function of the stimulation rate. Cochlear implant researchers currently do not fully understand why this is the case. Therefore, the complex interaction between stimulation rate and the wide range of patient outcomes suggests the need for a more refined comprehension of the neurophysiological mechanisms that modulate the response of spiral ganglion neurons to high stimulation rates. This paper describes several features of neural responses that may help us develop a much better understanding of this behavior.

We have an impoverished understanding of SGN excitability in response to high rates of stimulation chiefly due to the greater occurrence of temporal interactions for short interpulse intervals. In actuality, the SGN response will be determined by membrane

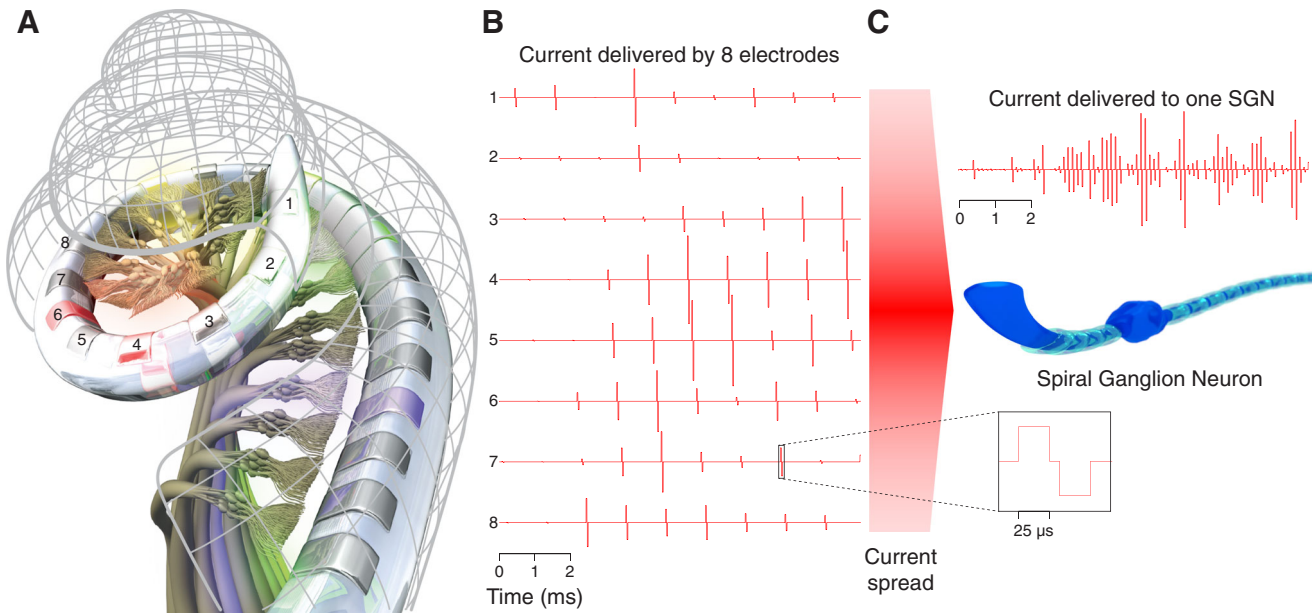


FIG. 1. Illustration of effective pulse rates for electrical stimulation of spiral ganglion neurons (SGNs) by a cochlear implant. **A** The positioning of an electrode array inserted into the cochlea (drawn as the gray mesh wireframe) relative to the SGNs that form the auditory nerve. It is desirable for stimulating electrical currents from different electrodes or electrode pairs (highlighted blue, green, yellow, and red) to maximally stimulate distinct subpopulations of SGNs (also highlighted correspondingly with blue, green, yellow, and red), such that the tonotopic arrangement of SGNs is utilized in transmitting information about different sound frequencies. However, in practice, there is substantial current spread along the length of the cochlea, such that a single SGN is subjected to a weighted sum of the currents delivered by the nearby

electrodes. For example, plotted in **B** are current pulse trains delivered by electrodes 1–8 for a short speech segment encoded at a rate of 900 pulses/s on each electrode. **C** An electrode separation of 1.4 mm and a monopolar stimulation attenuation of 0.5 dB/mm (Merzenich and White 1977) translate to the current spread profile (shaded red) that smears the contribution of all 8 electrodes to an example SGN situated between electrodes 4 and 5. This compound stimulation of an SGN results in an effective pulse rate that is much higher than the single-electrode rate of 900 pulses/s. Each biphasic pulse has a duration of 25 μ s/phase and a gap of 8 μ s between positive and negative phases. Image in **A** courtesy of Cochlear Americas, © 2015, adapted from Gray's Anatomy textbook.

capacitance and the types of voltage-gated ion channels that reside in its membrane. However, it is beneficial to characterize the resulting effects of these mechanisms in terms of stereotypical stimulus-response phenomena. Four phenomena that have been identified as occurring to varying degrees for the majority of excitable cells are refractoriness, facilitation, accommodation, and spike rate adaptation. These phenomena are also produced in type I SGN when stimulated by a CI. At high rates of stimulation, all of these behaviors are important and are interacting factors that regulate the firing pattern, whereas some are non-factors at low rates.

Figure 2 gives a single-trial stimulus-response overview of the phenomena of interest. The voltage traces in Figure 2A–D were generated from an SGN membrane model (Negm and Bruce 2014) with updated hyperpolarization-activated cyclic nucleotide-gated cation (HCN) kinetics (Liu et al. 2014b). It should be kept in mind throughout that multiple trials are necessary to capture the mean and variance of the response arising from the stochastic nature of action potential generation. Nevertheless, it is useful to visualize a representative membrane potential response to each stimulus pattern. The stimuli used in Figure 2A–C are typically referred to as either masker-probe (first-second) or paired-pulse paradigms, which are commonly employed to investigate refractoriness, facilitation, and accommodation. The purpose of this type of stimulation is to systematically determine how the neuron responds after a pre-conditioning stimulus. The response to the two pulses in Figure 2A is typical of a neuron in a refractory state, i.e., refractoriness, which is defined as a neuron's reluctance to spike twice in rapid succession. In order for refractoriness to be considered possible, the neuron must spike in response to the first pulse. In this example, the second pulse does not elicit an action potential from the neuron even though the second pulse has an amplitude well above the resting threshold current because it is still recovering from the first pulse and thus is said to be in a refractory state. Facilitation typically occurs, as shown in Figure 2B, when the masker-probe interval is small and both pulses are below the average threshold current. Effectively, this causes the first pulse to not generate a spike, but since the membrane potential remains near threshold long enough, the second pulse can push the membrane potential beyond threshold, resulting in a spike. Sometimes referred to as subthreshold adaptation (Brette and Gerstner 2005), accommodation also occurs when there is a subthreshold response to the masker pulse, but unlike facilitation, this leads to reduced excitability for the probe pulse response. When the masker-probe interval

is so large as to allow the membrane potential to decay back near or below rest, then in addition to a lack of facilitation, it is sometimes observed that the membrane excitability is suppressed for a short time. This can result in the probe pulse insufficiently exciting the neuron to trigger a spike even though the second pulse amplitude is above the resting threshold current, as shown in Figure 2C. Moving beyond the masker-probe stimulus paradigm, when a neuron is exposed to an ongoing pulse train, spike rate adaptation can occur in some neurons such that the spike rate decreases over time, even more than can be explained by refractoriness. This form of adaptation is distinct from accommodation in that spike rate adaptation is dependent on ongoing spiking (Benda and Herz 2003; Brette and Gerstner 2005). Over multiple trials, the spike rate can be determined by averaging the number of spikes occurring within a time interval. Figure 2D shows the membrane potential response to one trial in which the neuron progressively loses its ability to spike for every pulse.

The degree of refractoriness, facilitation, and accommodation (or their functions) can be mapped by using a paired-pulse (or masker-probe) paradigm by varying the levels of each pulse and the lag between them. Several experiments have been successful at measuring the refractory function, which shows the recovery in response to the second pulse given a spike in response to the first pulse. Facilitation and accommodation are described by the likelihood of a spike to occur in response to the probe pulse, given a subthreshold response to the masker pulse. Essentially, when the neuron constructively uses both pulses to produce one spike, it is referred to as facilitation, otherwise, when both pulses work to effectively desensitize the neuron, producing no spikes, we call this accommodation. However, the effects of facilitation and accommodation may be greater in response to pulse train stimulation compared to a paired-pulse response due to accumulation of the effects over the duration of the pulse train. Finally, spike rate adaptation is the neuron's tendency to lower its excitability in response to its prior spiking activity, i.e., spikes occurring before the immediately preceding spike. Taken together, it is easy to formulate scenarios in which more than one or all four behaviors simultaneously overlap (see Fig. 3E). Data illustrating these phenomena have been available in the literature for more than a decade in some cases (see the following section), yet physiological and perceptual data are often interpreted in light of refractoriness alone, with the other three stimulus-response phenomena not taken properly into

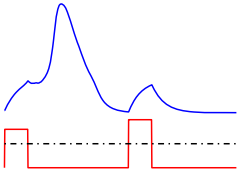
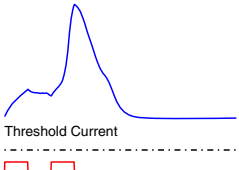
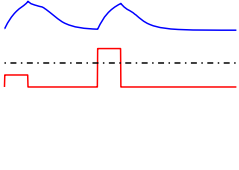
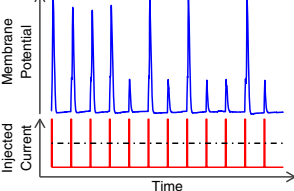
Phenomenon	Mechanisms	Reference
A Refractoriness 	Dominant effects <ul style="list-style-type: none"> - Absolute Refractory Period (ARP): Na channel inactivation, higher conductance of delayed-rectifier K channel - Relative Refractory Period (RRP): Na channel inactivation Secondary effects <ul style="list-style-type: none"> - HCN and KLT channels contribute to extending ARP - KLT channels lengthen the RRP - Rapidly activating, transient K_F current shortens RRP 	Hodgkin and Huxley (1952); Matsuoka et al (2001) Hodgkin and Huxley (1952); Matsuoka et al (2001)
B Facilitation (Temporal Summation) 	Passive effects <ul style="list-style-type: none"> - Capacitive charging of membrane towards threshold potential Active effects <ul style="list-style-type: none"> - Residual Na activation increases excitability to next pulse 	Lapicque (1907) Hodgkin (1938); Hodgkin and Huxley (1952)
C Accommodation (Subthreshold Adaptation) 	General mechanisms <ul style="list-style-type: none"> - Subthreshold adaptive exponential IAF model - Na channel inactivation Ionic channel contributions in SGN <ul style="list-style-type: none"> - HCN channels: fewer open channels with ongoing subthreshold pulse train - HCN channels: hyperpolarization with depolarizing pulses leads to regulation of the RMP - KLT channel activation and extracellular K^+ accumulation 	Brette and Gerstner (2005) Frankenhaeuser and Vallbo (1965) Negm and Bruce (2014) Liu et al (2014) Miller et al (2011)
D Spike–Rate Adaptation (Spike–Dependent) 	General mechanisms <ul style="list-style-type: none"> - Spike-triggered adaptive exponential IAF model - M-type currents: high-threshold K channels - Afterhyperpolarization-type current - Fast Na current: slow recovery from inactivation Ionic channel contributions in SGN <ul style="list-style-type: none"> - HCN channels: accumulating afterhyperpolarization - Extracellular K^+ accumulation 	Benda and Herz (2003) Brette and Gerstner (2005) Brown and Adams (1980) Madison and Nicoll (1984) Fleidervish et al (1996) Negm and Bruce (2014) Baylor and Nicholls (1969); Woo et al (2009a,b,c)

FIG. 2. Stimulus-response phenomena and their associated mechanisms. The *left column* (Phenomenon) shows sample SGN membrane potentials (*blue*) in response to monophasic current pulses (*red*) representing the different phenomena. These were generated with a Hodgkin–Huxley-type SGN membrane model (Negm and Bruce 2014). The *horizontal black dot-dashed line* indicates the resting threshold current for the SGN model. Possible responsible mechanisms for each are listed in the *middle column* (Mechanisms), with the source listed in the *right column* (Reference). Note that each panel (**A–D**) represents one trial outcome, and in general, many trials are required to characterize each behavior due to the stochastic nature of the membrane potential and thus the resulting spiking. **A** Refractoriness appears as reduced excitability to the second pulse given a spike in response to the first pulse, whereas at longer

interpulse intervals, a second spike is more probable. **B** Facilitation acts as membrane integration of two subthreshold pulses at small interpulse intervals to enable an action potential in response to the second pulse, whereas in the case of **C** accommodation, the states of some ion channels are responsible for reducing excitability after a subthreshold masker pulse such that an action potential may not be generated in response to a following pulse above the resting threshold current. **D** In response to ongoing spiking due to pulse train stimulation, spike rate adaptation refers to the diminished spiking activity over longer timescales than refractoriness. *HCN* hyperpolarization-activated cyclic nucleotide-gated, *KLT* low-threshold potassium, *IAF* integrate-and-fire, *RMP* resting membrane potential.

consideration. In this review article, we will present the current state of methods which quantify each behavior's

contribution to SGN activity and the respective emerging biophysical mechanisms.

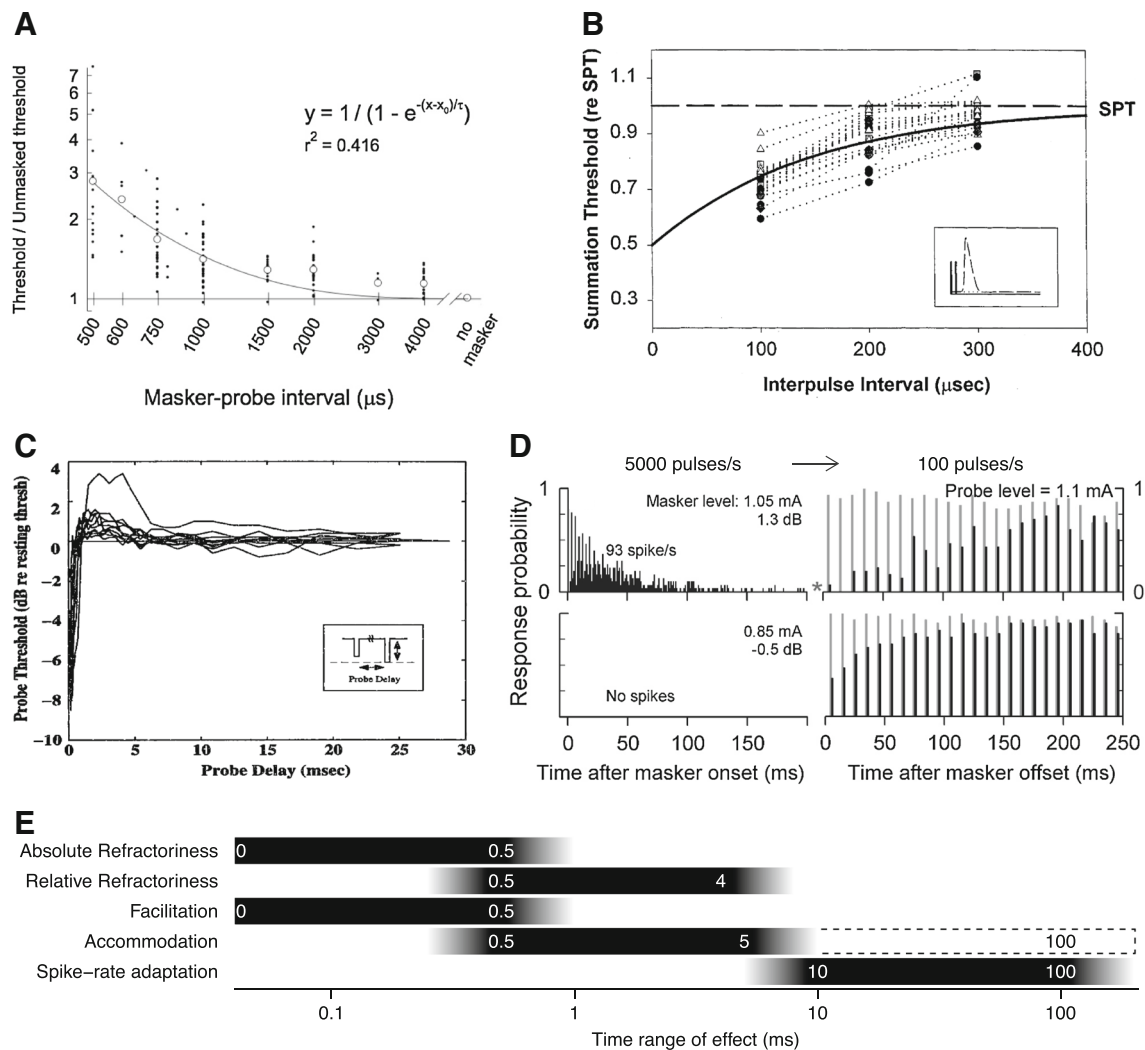


FIG. 3. Published data from cat SGN recordings illustrating the four stimulus-response phenomena: **A** refractoriness, **B** facilitation, **C** accommodation, and **D** spike rate adaptation, and **E** a summary of the timescale ranges of their operation. Data in panels **A–C** were collected with monophasic pulses, while the data in panel **D** were in response to biphasic pulses. Data in panels **A–C** were obtained with masker-probe pairs of pulses at a range of intervals, and the responses were characterized by the ratio of the threshold current for the second (probe) pulse to the single-pulse threshold (SPT; also referred to as the unmasked or resting threshold). **A** To determine the absolute and relative refractory behavior, only cases when the masker pulse elicits a spike are considered. Elevated probe pulse thresholds due to refractoriness are shown for multiple SGNs (solid dots) and their average (open circles) is fitted by the function (black line) with the equation given. **B** Reduced probe pulse thresholds due to facilitation are observed in the range of 100 to 300 μs . Data are shown for multiple SGNs and their average is fitted by an exponential function. **C** Both facilitation and accommodation were observed by using a masker-probe stimulation protocol including longer interpulse intervals. The masker pulse is set to levels of 2 to 0.5 dB below the single-pulse threshold, while the level of the delayed probe is varied. Accommodation is seen at probe threshold values greater than 0 dB, whereas facilitation occurs below 0 dB. **D** Responses to a masker train (left panels, stimulating at a rate of 5000 pulses/s) and following responses to a probe train (right panels, stimulating at 100 pulses/s) displayed using normalized post-stimulus time histograms. Probe responses (shown in the right panels) are

displayed as *black bars* if preconditioned with a masker train; otherwise, they are displayed as *gray bars*. In the *top-left panel*, the masker train is delivered with a constant pulse current level, substantially above the SPT, whereas in the *bottom-left panel*, the masker train is delivered with a subthreshold current level. In all conditions, probe trains are set to a constant current level, close to threshold. Reduced excitability to the start of the probe train is observed for both the suprathreshold masker (*top-right panel*) and the subthreshold masker (*bottom-right panel*) compared to the cases with no masker train. The *bottom-left panel case* is indicative of accommodation while the *top-left panel case* may include the combined effects of spike rate adaptation and accommodation. **E** The time ranges that refractoriness, facilitation, accommodation, and spike rate adaptation operate at are shown as *black bars*. The *black-to-white gradients* indicate the variability in the time ranges. The *white bar outlined by a dashed black line* represents the time range of accumulated accommodation in response to pulse train stimulation shown in panel **D**. Panel **A** reprinted with kind permission of Springer Science & Business Media: Fig. 7 from Miller et al. (2001), © 2001. Panel **B** reprinted with kind permission of Elsevier: Fig. 5 from Cartee et al. (2000), © 2000. Panel **C** is used with permission from Fig. 3-2 of Dynes (1996). © Massachusetts Institute of Technology. Panel **D** adapted with kind permission of Springer Science & Business Media: Fig. 1 from (Miller et al. 2011), © 2011.

STIMULUS-RESPONSE PHENOMENA

Refractoriness

In healthy SGNs, refractoriness is actually a feature which enhances spike timing precision (Avisar et al. 2013). Yet, even though SGNs have one of the fastest post-spike recoveries (Cartee et al. 2000; Miller et al. 2001; Cartee et al. 2006; Rattay et al. 2013), when CIs are involved, refractoriness can be perceived as a limitation of the maximum firing rate in response to pulse rates of 2000 pulses/s or higher.

Just over a century has passed since refractoriness was discovered in nervous and cardiac tissue (Tait 1910). At that point, it was described with an operational definition as a period of reduced excitability immediately following an action potential. Figure 2A demonstrates this concept by a single trial of a neuron's membrane potential that is unable to spike in response to the second pulse. This operational definition of refractoriness significantly predates the discovery of voltage-gated ion channels and their dynamics that give rise to refractoriness (Hodgkin and Huxley 1952).

Specifically, the refractory period is broken into an absolute refractory period (ARP) followed by a relative refractory period (RRP). The absolute refractory period is an interval of time which begins immediately following a spike when the neuron has a zero probability of spiking again to a second pulse of any magnitude. Following this “dead-time,” the relative refractory period is the interval of time where the elevated threshold for spiking eventually returns to the single-pulse threshold. The effect of this temporary threshold increase and recovery on the response to a stimulus of a fixed current amplitude translates to a spiking probability throughout the course of the RRP that begins at 0, which eventually returns to the single-pulse discharge probability.

Due to the stochastic nature of the type I SGN, multiple trials of spikes responding to pulses must be averaged to characterize the refractory function. Numerous groups have done work to extract the refractory function of the auditory nerve from spike train data in response to an ongoing pulse train (Miller 1985; Bi 1989; Miller and Mark 1992; Mark and Miller 1992; June and Young 1993; Prijs et al. 1993). However, this approach had limitations for practical CI stimulation strategies since it failed to take into account the pulse current level by only delivering pulse trains with constant level. In efforts to address this issue, Dynes (1996), Cartee et al. (2000), and Miller et al. (2001) have used a two-pulse masker-probe paradigm to map out the refractory function. For example, shown in Figure 3A is the result of using a masker-probe stimulus paradigm to uncover the refractory function. Miller et al. (2001) accomplished

this by first determining the single-pulse threshold (SPT) which, gathered over numerous trials, is the current level at which the neuron fires 50 % of the time to a pulse while the neuron is at rest. A measure of the magnitude of the neuron's stochastic activity and dynamic range can also be calculated and is referred to as the relative spread (Verveen 1961; Bruce et al. 1999). The masker-probe stimuli can then be delivered with a suprathreshold masker pulse and a variable level probe pulse separated by some masker-pulse interval. After independently varying both the probe current level and the masker-probe interval for multiple trials each, the refractory function can be expressed as a ratio of the probe threshold to the single-pulse threshold.

Data from several single-neuron recordings in cats were fit to a function (shown in Fig. 3A) to extract the absolute and relative refractory periods. From this data, they found mean values for the ARP of 0.33 ms and the RRP time constant of 0.41 ms. Cartee et al. (2000) produced a value of 0.7 ms for the RRP time constant by pooling data from all cells in their recordings, also in cats. However, this value is confounded with the ARP since compared with the Miller et al. (2001) study, Cartee et al. (2000) did not specify an ARP value in their refractory function fit. Parameter extraction from the refractory function is difficult and the outcome may lead to uncertain results. Parameter estimates are sensitive to the number of data points, the masker-probe interval axis values, the initial guesses for the parameters, and any constraints on the parameters in the fitting procedure.

Although not explicitly stated by Miller et al. (2001), Figure 3A shows a sizable proportion of neurons with relative refractoriness extending from 2 to 4 ms or greater and the refractory function fit undershoots the mean data points in that range. Similarly, in Cartee et al. (2000), the refractory function fit underestimates the mean data points from 2 to 3 ms (see Fig. 7 from Cartee et al. 2000). This longer timescale of relative refractoriness translates to a reduced neural excitability at pulse rates over 250 Hz. Protracted refractory periods have also been found in humans with CIs (Botros and Psarros 2010; Cohen 2009) using electrically evoked compound action potential (ECAP) measurements.

Facilitation and Accommodation

To the best of our knowledge, Lucas (1910) introduced the concept of two monophasic subthreshold pulses, separated by a “summation interval” working to produce an action potential in response to the second pulse. The use of the term summation has persisted in several papers (Cartee et al. 2000; Cartee et al. 2006), whereas Dynes (1996) named it sensitiza-

tion. In this context, summation refers to temporal summation. This is different from spatial summation that describes the addition of numerous postsynaptic potentials (Kandel et al. 2000). To remove the ambiguity between temporal summation and spatial summation in this paper, we will adopt the term facilitation, which has been used previously in the literature to describe temporal summation (Heffer et al. 2010; Cohen 2009; White 1984). The term accommodation was used by Sly et al. (2007) and Heffer (2010) but has also been referred to as desensitization (Dynes 1996) and inhibition (Cohen 2009). However, we will persist with the historical nomenclature, namely accommodation which was introduced by Nernst (1908) and later developed further (Hill 1936; Katz 1936; Solandt 1936) to describe how the membrane responds to a slowly changing stimulus current. Some of these earlier studies focused on one ramp stimulus, but in the context of CI stimulation, the issue of multiple pulses and how they precondition future pulses is more appropriate.

Phenomenologically, facilitation and accommodation represent two sides of the same coin when applied to CI stimulation. Following a subthreshold response to a masker pulse, the neuron can build on its depolarized membrane potential in order to facilitate an action potential in combination with the next pulse (Fig. 2B). Alternatively, it can accommodate to the masker pulse causing reduced excitability to the probe pulse. The reduced excitability is caused by the state of various ion channels following the response to the masker pulse (Fig. 2C). These definitions apply to typical single-trial responses of masker-probe stimuli but vary to some extent due to stochastic membrane activity. Similar to the masker-probe stimuli methodology used for establishing the refractory function, multiple trials are necessary for characterizing the facilitation and accommodation functions in terms of threshold ratios.

Facilitation. By setting both masker and probe pulses to a current level of 5 % below threshold and varying the masker-probe interval, Lucas (1910) found a value of masker-probe interval which facilitated spiking in frog muscle tissue. More recently, Heffer et al. (2010) used biphasic pulse trains with stimulation rates between 200 to 5000 pulses/s at current levels corresponding to low-, medium-, and high-onset spike probabilities to investigate facilitation in the auditory nerve. They could estimate the effect of facilitation as the increase in spiking probability from a single pulse to a pulse train in a 2 ms window, while capping the spike count at 1. Consistent with the subthreshold notion of facilitation, they found that facilitation occurred predominantly at the low-spike-onset probabilities and increased as a function of the stimulation rate. As an

improvement to the Lucas (1910) study, Cartee et al. (2000, 2006) expanded the experiment by concurrently varying the masker and probe current levels in single-neuron recordings of feline type I SGN. Cartee et al. (2000, 2006) computed the summation (facilitation) threshold relative to the SPT by stimulating with charge-balanced pseudo-monophasic masker-probe pulses in a fashion similar to that employed by (Miller et al. 2001) for determining their refractory function. Technically, the only difference between the procedures was that as the pulse levels were varied to extract the threshold for a given masker-probe interval, Cartee et al. (2000, 2006) set both masker and probe pulses to equal current amplitudes. Figure 3B shows how this allowed for a functional description of facilitation in the tested range of 100 to 300 μ s. The facilitation model was assumed to be equal to half of the single-pulse threshold at a masker-probe interval of 0 μ s, since both pulses would simply add. As the masker-probe interval increased, the effect of facilitation diminished and eventually tended towards the single-pulse threshold. A caveat of the Cartee et al. (2000) study was the assumption that both masker and probe pulses were linearly additive in type I SGNs. Upon closer examination of Figure 3B, since a subset of the SGNs at 300 μ s had thresholds that were greater than the single-pulse threshold, this notion is violated. Although Cartee et al. (2000) attributed this anomaly to an SGN threshold shift during the data collection procedure, an alternative explanation is that accommodation is responsible (Dynes 1996; Sly et al. 2007).

Accommodation. For cases of reduced neural excitability at short timescales, instances of accommodation are sparse in the refractory-dominated CI literature despite being well known in neuroscience. In a similar experimental protocol to Cartee et al. (2000, 2006), Dynes (1996) found evidence of the coexistence of facilitation and accommodation by significantly expanding the maximum masker-probe interval out to 25 ms. Figure 3C illustrates this point clearly, with data from 10 neurons in 4 different cats and by using a monophasic masker-probe paradigm. Specifically, masker levels were 2 to 0.5 dB lower than the SPT (i.e., where the discharge probability equals 0.5) and a tracking algorithm was employed to determine the probe threshold at all masker-probe interval values. Facilitation is said to occur when the probe threshold was less than 0 dB with respect to the SPT. In Figure 3C, facilitation is observed below 0.5 to 1 ms, whereas when the masker-probe interval took on values between 1 and 5 to 10 ms, accommodation occurred. Here, the mean probe threshold was 1 dB greater than the single-pulse threshold. Finally, the return to the SPT at large masker-probe intervals is an indicator that the temporal interactions imposed on

the membrane potential by the pulses is no longer in effect and the subthreshold responses may be considered independent. Given that we know the shape of the facilitation function (Cartee et al., 2000, 2006) and the combined effects of facilitation and accommodation (see Fig. 3C, E), it may be possible to obtain a separate accommodation function by using a subtractive fitting procedure.

Another instance of what could be interpreted as accommodation was reported for two subjects by Cohen (2009) in human biphasic CI stimulation with ECAP recording. In these two instances, accommodation was observed over the 0 to 6 ms masker-probe interval. Current levels were 20 % for the probe pulse and slightly larger for the masker, nevertheless still below the 50 % current level (see Figs. S3 and S4 of Cohen 2009). Using single-neuron recordings in deafened guinea pig and stimulating with trains of 200 pulses/s, Sly et al. (2007) also found evidence of accommodation that occurred at all levels of subthreshold current. In the next section, we will also discuss accommodation and how it can be misunderstood as spike rate adaptation.

Spike Rate Adaptation and Interacting Phenomena

Neural adaptation is a widely observed response seen in sensory systems. Its function is thought to remove redundant information and conserve energy. In this context, spike rate adaptation is thought to be one of the possible mechanisms by which neural adaptation occurs. More specifically, spike rate adaptation is a neuron's tendency to lower its excitability in response to ongoing action potentials. This is generally observed across timescales on the order of 10 to 100 ms (Zhang et al. 2007; Heffer et al. 2010; Miller et al. 2011) or even minutes (Litvak et al. 2003) but typically greater than those for refractoriness, facilitation, and accommodation. For example, one trial of a neuron's response to high-rate stimulation in Figure 2D shows that initially, the neuron fires multiple consecutive action potentials, then later in the pulse train, the occurrence of spikes diminishes. Therefore, the neuron is said to be adapting its spike rate. A neuron's spike rate can be quantified simply with a post-stimulus time histogram (PSTH) by counting the number of spikes occurring in a time bin, dividing by the width of that bin, and then averaging over multiple trials. A naive assumption is that one can directly estimate the degree of spike rate adaptation from a PSTH. However, as we have seen in previous sections, the neuron's refractoriness, facilitation, and accommodation can also contribute to the shape of the PSTH, especially at small timescales (or high stimulation rates).

Zhang et al. (2007) explored effects on the spike rate by applying pulse trains at various stimulation rates and current levels to cat SGNs. Generally, the shape of the PSTHs across all conditions was described by a decay from an initial maximum spike rate towards a stabilized lower spike rate. The exception to these canonical PSTHs appeared in the case where neurons responded to the 10,000 pulses/s pulse train for a current level lower than the SPT. Beyond some initial spiking activity, the final spike rate reached 0 spikes/s (see the upper-rightmost panel of Fig. 2 of Zhang et al. 2007), which implied an ongoing accommodation to the subthreshold pulse train.

In a follow-up study, Miller et al. (2011) investigated both the buildup of and the recovery from adaptation. The stimulation paradigm involved applying a "masker" pulse train to induce adaptation and immediately after the cessation of the masker to switch to a low-rate "probe" pulse train, in order to observe the recovery from adaptation. Figure 3D shows two particularly different cases: illustrating that either suprathreshold or subthreshold masker pulse trains can reduce excitability to future probe pulse trains. In the top-left panel of Figure 3D, a suprathreshold masker pulse train at 5000 pulses/s elicits a slowly decaying spike rate (black bars) over a 200 ms interval, which, on the surface, appears to be spike rate adaptation. The top-right panel of Figure 3D shows what happens when the pulse rate subsequently drops to 100 pulses/s for the probe pulse train, which had a near-threshold current level: the spikes rate (black bars) remains near zero for the first two pulses and then the spike rate gradually increases back towards the unmasked spike rate (shown by the gray bars) over a period of around 200 ms. Thus, the buildup of spike rate adaptation and recovery from that adaptation appears to occur on similar time scales of 10s to 100s of milliseconds. In the bottom panels of Figure 3D, this stimulus paradigm is replicated but with the masker pulse train at a subthreshold current level, which leads to generating no action potentials during this interval.

Despite the lack of spikes to the 5000 pulses/s subthreshold masker train (bottom-left panel of Fig. 3D), when the pulse rate switches to 100 pulses/s for the probe pulse train, the spike rate (black bars in the bottom-right panel of Fig. 3D) is again reduced relative to the unmasked spike rate (gray bars) and takes around 100 ms to recover. It thus appears that *accommodation* was accumulating during the 200 ms of the high-rate masker pulse train, and it took the SGN some time to recover from this accommodation once the pulse rate dropped to 100 pulses/s for the probe pulse train. This suggests that such a level of baseline recovery that is attributed to accommodation seen

here in the bottom panels of Figure 3D could also be present along with the spike rate adaptation shown in the top panels of Figure 3D. Refractoriness also makes an appearance in the top-left panel of Figure 3D, for pulse train onset times less than 25 ms, in the form of the oscillatory response, whereas the spike rate adaptation component of the normalized PSTH is its slowly decaying envelope.

Studies by Litvak et al. (2001) and Heffer (2010) have reported on accommodation in response to biphasic pulse trains. The results of similar experiments by Zhang et al. (2007) also showed evidence of reduced excitability due to subthreshold responses although it was not explicitly stated by the authors. True spike rate adaptation should only depend on the onset spike rate. However, Zhang et al. (2007) found that greater spike rate decrements occurred for higher pulse rates at equal onset spike rate (see Fig. 5D–I of that article). In fact, all three experimental studies (Litvak et al. 2001; Heffer 2010; Zhang et al. 2007) showed that the normalized spike rate decrement (or spike reduction ratio) increased concomitantly with stimulus frequency. This indicates that accommodation is contributing to the spike rate decrement in parallel to spike rate adaptation.

Due to the simultaneous interaction of refractoriness, facilitation, accommodation, and spike rate adaption, several groups have proposed computational methods to disentangle the contributions of a subset of stimulus-response phenomena to the total spike rate. Using similar techniques, Trevino et al. (2010) and Plourde et al. (2011) were able to extract a rudimentary refractory function (i.e., low temporal resolution) from the neuron's spiking history given an acoustic stimulus, but this framework could easily be extended for electrical stimulation. Campbell et al. (2012) were also able to delineate between the effects of refractoriness and spike rate adaptation using constant and variable pulse train amplitudes. Similar work has been done to predict the effect of accommodation and refractoriness on the spiking pattern (Goldwyn et al. 2012). However, spike rate adaptation was not addressed. Thus, to date, there have been several attempts to mathematically separate subsets of the four stimulus-response phenomena, but it remains to develop a mathematical methodology for fully isolating all four phenomena from a set of spike trains. Future methods which attempt to separate the effects of facilitation and/or accommodation from the spike rate must consider the current level of the stimulus pulse train. This is in contrast to refractoriness and spike rate adaption which can be detected from spiking only.

MECHANISMS AND MODELS

In parallel to the subthreshold and suprathreshold type I SGN phenomena we have just discussed, insights into the mechanisms responsible for these phenomena have begun to take shape with the help of relatively recent electrophysiology and computational modeling work. Historically, Hodgkin and Huxley (1952) laid the groundwork for mechanisms of action potential depolarization, repolarization, and fast afterhyperpolarization in squid giant axon. In their model, the principle ionic currents were formed by the fast sodium and delayed rectifier potassium voltage-gated ion channels. To this day, these channels are central to explaining the biophysical underpinnings of neural excitation in the SGN and thus are used in many computational models (Phan et al. 1994; Rubinstein 1995; Matsuoka et al. 2001; Mino et al. 2004; Imennov and Rubinstein 2009; Chow and White 1996; Negm and Bruce 2014; Negm and Bruce 2008; Woo et al. 2009b; Woo et al. 2009a; Woo et al. 2009c; Miller et al. 2011; Smit et al. 2008; Cartee 2000, 2006; Rattay 2000; Rattay et al. 2001; Rattay et al. 2013; Rattay and Danner 2014). However, the ion channels of the Hodgkin–Huxley model alone cannot explain long relative refractoriness, long-term accommodation, and spike rate adaptation.

Research has begun to address the effect of CI stimulation in mammalian auditory systems by using more biologically realistic information and models. In doing so, a remarkable diversity of voltage-gated ion channel types have been revealed in type I SGNs. To follow up on the Hodgkin–Huxley sodium channels, a modern survey of the type I SGN in mice revealed Nav1.6 channel subunits located at all nodes of Ranvier with particularly higher densities at the unmyelinated afferent process innervating the IHC layer and the nodes flanking the soma (Hossain et al. 2005). In end-stage postnatal development murine type I SGN, Adamson et al. (2002) found several potassium channel subunits. Specifically, the high-frequency basal neurons were dominated by high-threshold fast-delayed rectifier Kv3.1, low-threshold Kv1.1, and calcium-activated K⁺ subunits, while the low-frequency apical neurons showed a majority of inactivating Kv4.2 subunits known for extending the latency of spiking near threshold.

Of particular importance to the SGN response phenomena are the Kv1.1 and Kv1.2 low-threshold potassium (KLT) and hyperpolarization-activated cyclic nucleotide-gated cation (HCN) channel subunits. The kinetics of both channel types operate at slower timescales than the Hodgkin–Huxley channels (Rothman and Manis 2003; Liu et al. 2014b). KLT channels are responsible for increasing the cell's voltage threshold and hyperpolarizing the resting

membrane potential (Liu et al. 2014a). HCN channels are well known for being permeable to Na^+ and K^+ with ratios ranging from 1:3 to 1:5 (Biel et al. 2009). When HCN is activated under membrane hyperpolarization, this generates a dominant inward Na^+ current which helps return the membrane potential back towards rest. HCN channels contribute to stabilizing the resting membrane potential of SGNs (Liu et al. 2014a; Liu et al. 2014b), a function that HCN appears to fulfill in a range of different cell types (Robinson and Siegelbaum 2003; Howells et al. 2012; Benarroch 2013). An interesting property of the current produced by HCN channels, known as I_h , is that it can increase the neuron's firing by a rebound excitation which happens towards the end of a hyperpolarizing pulse (Chen 1997).

Recently, Yi et al. (2010) complemented the (Hossain et al. 2005) Nav1.6 subunit localization of HCN subunits in rat type I SGN. Figure 4 shows the HCN1 and HCN4 subunits at nodes surrounding the soma and the first peripheral node. Although it remains unclear where the KLT channels in type I SGN are located, several studies have shown that they are indeed present. Kv1.2 subunits were found on axons of rat type I SGNs projecting to the anteroventral cochlear nucleus (Bortone et al. 2006). Mo et al. (2002) found Kv1.1 subunits on cell bodies and axons of type I SGN in mice. Again in mice, Reid et al. (2004) found differential densities of $\alpha\text{-Kv1.1}$ subunits along the cochlea. Type I SGNs in the basal cochlear region showed a greater expression than those in the apical regions. A better understanding of the localization of KLT channels in other sensory systems may serve as a starting point for investigation in type I SGNs. For example, in mammalian retinal ganglion neurons, reviews of voltage-gated ion channels by Rasband and Shrager (2000) and Lai and Jan

(2006) unambiguously show that Kv1.1 and Kv1.2 subunits, responsible for the low-threshold potassium current, cluster on the cell membrane in the region under the myelin sheath but proximal to the node of Ranvier, otherwise known as the juxtaparanode.

Refractoriness

Among the various definitions for refractoriness, neuroscience textbooks, e.g., Kandel et al. (2000), often portray the simplistic view that sodium channel inactivation is the cause. However, the SGN has multiple other ion channel types which also shape the cell's refractory properties. Because of this, it becomes infeasible to concisely describe refractoriness in terms of ion channel activity. This is where the first operational description that Tait (1910) offered is attractive. Several computational studies have augmented the Hodgkin–Huxley standard with additional channel types found in SGNs in order to understand their contribution to refractoriness given the results from mammalian CI studies.

Imennov and Rubinstein (2009) used a computational model of cat SGN axon embedded with the fast sodium channels, rapidly activating and transient potassium channels, and delayed rectifier channels. This combination yielded an absolute refractory period of 0.75 ms, which is longer than the range reported in Miller et al. (2001). Imennov and Rubinstein (2009) reported a relative refractory period of 5 ms, which is greater than the mean value of 442 μs Miller et al. (2001) produced, yet shows promise in terms of accounting for the long relative refractory period observed in a fraction of the SGNs (recall Fig. 3A). With a persistent sodium channel added to the temperature-modified Hodgkin–Huxley model of the human type I SGN, Smit et al. (2010) found

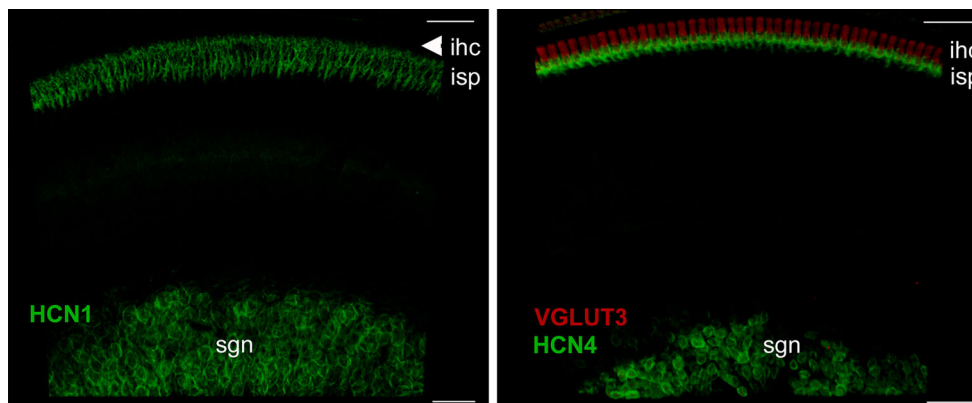


FIG. 4. Hyperpolarization-activated cyclic nucleotide-gated (HCN) channel subunit expression in rat cochlea identified on type I SGN. Labeled in green, both HCN1 and HCN4 subunits are localized to the nodes of Ranvier neighboring the cell body and the first peripheral node of Ranvier, or the inner

spiral plexus (ISP). Shown in red, vesicular glutamate transporter 3 (VGLUT3) was used to identify inner hair cells (IHCs). Reprinted with kind permission of the American Physiological Society: Fig. 4 from Yi et al. (2010), © 2010.

similar values for the ARP and RRP time constant of 0.8 and 3 ms, respectively. More recently, by using a node of Ranvier model of cat SGN with fast sodium and delayed rectifier channels, Negm and Bruce (2014) iteratively augmented the model with HCN and KLT channels. Even though the model variants could not explain cases of long relative refractoriness, they found ARPs in the same range to that of Miller et al. (2001), with 0.31 ms for the Hodgkin–Huxley channels only, 0.4 ms when both HCN and KLT were added, and intermediate values when only one channel type was added, although KLT produced the largest single change.

In general, biophysical neuron models use a bottom-up approach to predict higher-order emergent phenomena. It must be kept in mind that defining a model that can simultaneously predict refractoriness, facilitation, accommodation, and spike rate adaptation is often problematic due to the complexity that stems from a high dimensional parameter space exploration. A rather salient example of this issue is depicted in Fig. 6 of Miller et al. (2011). It shows that even after varying the densities of two unique potassium ion channel types, the model cannot successfully predict one ratio of densities that can simultaneously and accurately quantify refractoriness and spike rate adaptation in electrically stimulated SGNs.

Facilitation

One of the possible mechanisms for facilitation, i.e., the process of stimulating with sequential pulses thus leading to a spiking on the last pulse (see Fig. 2B), is through capacitive membrane charging. Conceptually, this can be understood with the venerable integrate-and-fire model (Lapicque 1907; Brunel and van Rossum 2007; Knight 1972; Burkitt 2006). If depolarizing monophasic pulses are separated by some time which is smaller than the membrane time constant, then the charge accumulated on the membrane from the first pulse will be too great to completely discharge before the membrane begins to integrate the next pulse. This process accumulates until the membrane potential reaches threshold and then fires. One of the caveats of relying solely on membrane charging to account for facilitation is that the charge across the membrane dissipates faster when the neuron is presented with the second hyperpolarizing phase of a biphasic pulse. This would diminish the accumulation of charge that would otherwise augment the effectiveness of the next pulse. However, experiments have shown that facilitation is also present in cases of biphasic pulse stimulation (Heffer et al. 2010; Cohen 2009) which implies that

there is an active agent that can at least partially suppress the hyperpolarizing phase.

A mechanism which could explain facilitation with either monophasic or biphasic stimulation relates to sodium activation near threshold (Hodgkin 1938). In cases where the membrane potential is near the threshold potential and the neuron does not produce an action potential, “residual” sodium activation can sustain the membrane potential near the threshold potential longer than the duration of the pulse, as illustrated in Figure 5 (see also Figs. 10–11 of Hodgkin 1938). Figure 5A compares membrane potential responses of a mammalian temperature-adjusted Hodgkin–Huxley model (Negm and Bruce 2014) stimulated by two monophasic pulses (Fig. 5C) in three different cases. Each trace shown is the average of 100 simulations for that particular case. The first case is that of a passive membrane response (black dot-dashed curve), for which the numbers of open ion channels are fixed at their resting values. This curve shows the passive charging up and decay of the membrane potential in response to the two pulses. In the second and third cases, the model ion channels were allowed to obey their prescribed voltage-dependent gating dynamics. The magenta curve corresponds to 100 trials in which the model SGN happened to *not* spike in response to the second pulse, whereas the green curve corresponds to 100 trials in which the model *did* spike to the second pulse. In both cases, the decay of the membrane potential back towards rest after the first (masker) pulse is slower than for the passive membrane, because of the action of the Na channels. Figure 5B shows the average percentage of open Na channels as a function of time. It can be observed that for the case where the model did spike (green curve), a greater number of sodium channels happened to open up in response to the depolarization from the first (masker) pulse when compared to the case where the model did not spike (magenta curve). The greater number of open Na channels led to a slower decay of the membrane potential during the interpulse interval and a higher residual membrane potential at the time of the second (probe) pulse, thus facilitating a spike. With regard to facilitation in response to trains of biphasic pulses, a Frankenhaeuser–Huxley model of a myelinated neuron mimicked (simulated) facilitation when stimulated with multiple biphasic conditioner pulses (see Fig. 8 of Butikofer and Lawrence 1979). Although they did not explicitly examine the mechanisms, sodium activation is most likely to be the major active factor responsible for facilitation in the study by Butikofer and Lawrence (1979). The evidence points to the response of the masker pulse lowering the threshold for the response to probe pulse as the pulses move closer together (see Fig. 3B) after

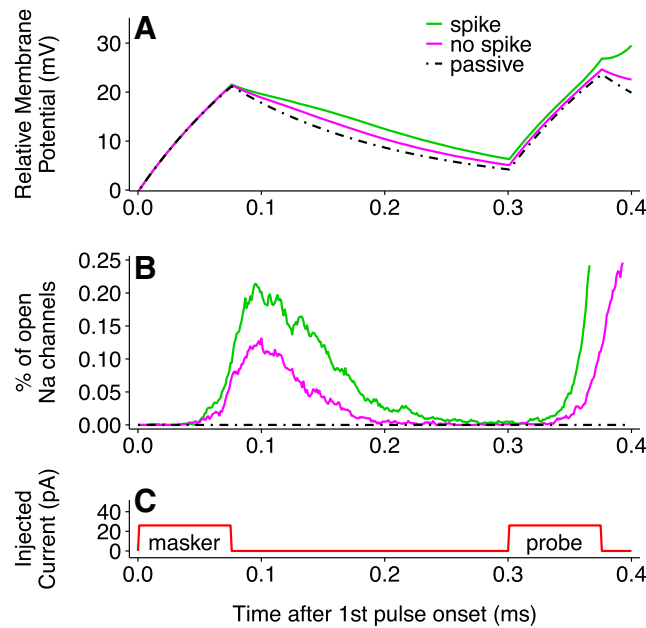


FIG. 5. Illustration of passive and active contributions to the facilitation (temporal summation) phenomenon, generated with a Hodgkin–Huxley-type SGN membrane model (Negm and Bruce 2014). **A** Relative membrane potential and **B** percentage of open Na channels responding to a **C** monophasic masker-probe stimulation paradigm with 75 μ s/phase pulse durations. Responses were averaged over 100 simulation trials for the relative membrane potential and percentage of open Na channels. Panels **A** and **B** show instances when the model SGN spiked (*green curve*) in response to the probe pulse, when it did not spike (*magenta curve*) in response to the second pulse, and where the fraction of

open ion channels were fixed at their resting values (passive response; *black, dot-dashed curve*). By comparing the cases of spiking versus no spiking, it is apparent that when the SGN spiked, it was caused by an increased number of Na channels flicking open in response to the first pulse, such that the membrane potential decayed back towards rest more slowly than it did for cases where the SGN did not spike. The increased depolarization of the membrane at the time when the second pulse is delivered contributes to greater facilitation than would be produced by the passive response.

conducting multiple trials to discern the average behavior of facilitation. Therefore, the effect of sustained subthreshold sodium activation buildup (active facilitation) combined with the capacitive membrane charging (passive facilitation) from multiple pulses makes the mechanism for facilitation easier to understand, although it is likely that sodium channel inactivation will limit the duration over which facilitation can accumulate.

Accommodation

As we have pointed out in “Facilitation and Accommodation,” there is a shortage of CI-related research on accommodation. Yet, as little as one subthreshold pulse can easily precondition responses of future stimuli such that they have elevated thresholds. Despite the subthreshold adaptation exhibited by some generalized mathematical models (Izhikevich 2003; Brette and Gerstner 2005), unfortunately biophysical mechanisms for accommodation are less well understood. However, one notable study gave some direction to accommodation in neurons with fast sodium and delayed rectifier potassium channels (Frankenhaeuser and Vallbo 1965). They found that

out of all parameters in a model of frog neuron, sodium inactivation correlated the highest with rapid accommodation. The involvement of sodium inactivation may have some explanatory power when the neuron spikes infrequently in response to pulse train stimuli due to residual sodium inactivation. However, sodium inactivation in response to a subthreshold masker pulse may not have sufficient strength and duration to fully explain the degree of accommodation experienced by the probe pulse in all cases.

Modern experimental studies have shown that several ion channel types may be implicated in generating currents that could further contribute to accommodation over a range of timescales, particularly beyond the timescale of sodium inactivation. For example, KLT channels show evidence of hyperpolarizing tail currents following subthreshold depolarizing voltage clamp pulses (see Fig. 8 of Rothman and Manis 2003) when their inactivation properties are taken into account. Further, a small but non-negligible, hyperpolarizing HCN conductance exists at voltages just above the resting membrane potential (RMP) of type I SGNs (see Fig. 6 of Liu et al. 2014b). Both of these instances drop the membrane potential below the RMP at the offset of depolarizing pulses

and, under these conditions, increase the threshold for the next pulse.

In a stochastic Hodgkin–Huxley model augmented with HCN channels, Negm and Bruce (2014) determined that the I_h current was involved in accommodation. The stimulation used was a 20-ms 2000 pulses/s biphasic pulse train at a constant current amplitude corresponding to a single-pulse spiking probability of 0.2. When only collecting the 20-ms trials that elicited no spikes, the interpulse membrane potential and the fraction of open HCN channels concomitantly experienced an ongoing drop in response to each successive subthreshold pulse. Over time, this leads to a lowered SGN excitability by distancing the membrane potential from threshold.

Spike Rate Adaptation

An effort to explicitly model spike rate adaptation for CI stimulation was developed in a series of papers by Miller et al. (2011) and Woo et al. (2009a, 2009b, 2009c). The idea was that during the repolarization of an action potential, K^+ ion efflux contributed to incrementally increasing the extracellular K^+ ion concentration. This would progressively shift the resting membrane potential to a more positive value, leading to sodium channel inactivation and thus reduce the excitability of the cell. Even though the models were successful for predicting spike rate adaptation in response to low and high rates of stimulation, the biophysical mechanism was taken from the leech central nervous system (Baylor and Nicholls 1969) and the applicability to mammalian auditory physiology remains in question.

One of the key findings on the cause of spike rate adaptation in the auditory system was found in a study by Mo et al. (2002). By injecting a constant current into rapidly adapting murine type I SGNs and blocking Kv1.1 channels, the neuron significantly increased its excitability. In another auditory neuron, namely neurons of the medial nucleus of the trapezoid body, Brew et al. (2003) also demonstrated elevated excitability in Kv1.1 subunit-deficient mice, compared to the wild-type and heterozygous variants. These findings motivated multiple groups to incorporate the KLT channels in their modeling of CI stimulation (Miller et al. 2011; Negm and Bruce 2008; Negm and Bruce 2014). Without using the extracellular potassium mechanism, Negm and Bruce (2008, 2014) simulated spike rate adaptation behavior by adding KLT and HCN channels to their computational node of Ranvier model. It was found that HCN affected the firing rate under stimulation rates ranging from low to high, whereas KLT only became a factor at the high stimulation rates.

Other possible contributors may explain reduced excitability to an ongoing stimulus. Sources include the sodium–potassium pump, which produces a slow afterhyperpolarization (Gulledge et al. 2013), channel mechanisms from different systems (Fleidervish et al. 1996; Madison and Nicoll 1984; Brown and Adams 1980), and several general models (Benda and Herz 2003; Brette and Gerstner 2005). However, further research is necessary to determine their applicability to type I SGNs.

SPATIAL EFFECTS OF CI STIMULATION RELATED TO TEMPORAL INTERACTIONS

The type I SGN response to CI stimulation is very different from its response to synaptic input from an IHC. The firing pattern of a single SGN when stimulated by a CI is the combined result of spatial and temporal interactions. Due to current spread, the SGN receives smeared pulse streams originating from multiple independent neighboring electrodes. While the strongest current is from the closest electrode, distal electrodes may impose a subthreshold influence on the SGN which can result in both facilitation and accommodation. The case of current spread illustrated in Figure 1B–C is applicable for cases of moderate-rate stimulation (in this illustration 900 pulses/s on each electrode) with pulse trains coming from nearby electrodes in a monopolar configuration (i.e., with the return electrode outside the cochlea). The types of patterns produced across the electrode array will depend on exactly which coding strategy is implemented in the CI sound processor (for a review of different approaches, see Loizou 1998), the mapping from acoustic frequency channels to electrodes (which varies from user to user), and the spectrum of the sound. The pattern of pulses in Figure 1B could potentially be produced by a broad spectral peak processed by a peak-based strategy such as the Advanced Combined Encoder or Spectral Peak schemes (ACE, SPeak; Cochlear Corp., Sydney, Australia), or alternatively by the Continuous Interleaved Sampling strategy (CIS; (Wilson et al. 1988; Wilson et al. 1993)) mapped to eight neighboring electrodes. To reduce the effects of current spread for a CIS strategy, the eight channels could be mapped to more widely spaced electrodes on the array. However, for monopolar stimulation, the current spread is so broad that the spatial summation is still likely to strongly affect the temporal interactions. Therefore, efforts to reduce current spread have been proposed that could lead to the reduction of subthreshold effects and the targeting of smaller subpopulations of SGNs per channel. Some promising methods are being developed for more accurately steering current towards the

intended SGNs, such as using bipolar, tripolar, or even multipolar electrode configurations (van den Honert and Kelsall 2007).

In addition to the issue of which SGN is stimulated by which current pulse, another concern for stimulation by a CI is the variability in the site of spike initiation, i.e., on which node of Ranvier for a particular SGN the spike is first generated. In the healthy acoustically driven ear, spikes are initiated at the peripheral terminal aided by a dense population of Nav1.6 channels (Hossain et al. 2005). The spike timing of the SGN inherits variability from the synaptic transmission process between an IHC that is characterized by probabilistic release of vesicles (Glowatzki and Fuchs 2002; Heil et al. 2007; Safieddine et al. 2012). However, the spike timing of the SGN is known to have intrinsic variability due to the inherent stochasticity of voltage-gated ion channel fluctuations (Verveen and Derksen 1968; Sigworth 1981). While smaller in magnitude than IHC vesicle release variability, the effect of ion channel fluctuations in SGNs is larger than for many other types of neurons since membrane noise is greater at small node of Ranvier diameters (Verveen 1962). So, in the case of cochlear implant stimulation, even with just one extracellular electrode, these same stochastic properties promote multiple locations on the SGN from where an action potential can originate (Rattay et al. 2001; Miller et al. 2003; Sly et al. 2007), in contrast to the reliable spike initiation at the peripheral terminal for synaptic transmission by an IHC. In a stochastic model of an SGN axon, Mino et al. (2004) demonstrated that spike timing variability was maximized near the single-pulse threshold current level and the spike initiation node exhibited a wider distribution as the electrode-to-axon distance increased. If the peripheral processes of SGNs begin to deteriorate following IHC loss (e.g., Hardie and Shepherd 1999, Webster and Webster 1981), then the nodes of Ranvier flanking the soma may serve as the predominant loci for CI-induced excitability since they also contain a relatively high density of Nav1.6 subunits (Hossain et al. 2005).

Furthermore, due to the underlying ion channel mechanisms, membrane potential responses are dependent on the polarity and the pulse shape of the stimulation. It is possible for anodic and cathodic pulse phases to cause different patterns of depolarization and hyperpolarization across the nodes of Ranvier in an SGN. For example, in the simplest case, by stimulating with monophasic pulses using computational models of cat and human SGNs, Rattay et al. (2001) demonstrated that while model cat SGNs were more easily excited with the cathodic polarity, model human nerves displayed greater sensitivity to the anodic pulse. This result was confirmed in humans with biphasic pulses (Macherey

et al. 2008). Therefore, care should be taken in generalizing across stimulation pulse type and species with respect to the response properties of refractoriness, facilitation, accommodation, and spike rate adaptation, because the site of action potential initiation or the patterns of subthreshold depolarizations and hyperpolarizations along an axon will be dependent on the exact electrode–neuron geometry and the pulse waveform.

CONCLUSIONS

We are still in the infancy of the type I SGN characterization of ion channel type and location across different species. As a result, different phenomena have been explored in different classes of SGNs ranging from the base to the apex of the cochlea and from low to high thresholds. More research must be done to determine if all four behaviors: refractoriness, facilitation, accommodation, and spike rate adaptation, can, in fact, be generated by a single type I SGN. Even though biphasic stimulation is clinically relevant, our understanding of the neural response to biphasic stimulation is impoverished compared to the monophasic response. In the interim, computational modeling could be an important way to relate in vivo electrophysiological data to possible ion channel distribution and determining if monophasic responses generalize to biphasic ones, or understanding the mechanisms, if they are different.

CIs are experiencing an interesting period in their development. Contemporary research is addressing methods of delivering stimulation from the CI to SGNs—all with the goal of improving speech perception in a variety of real-world settings. Many studies focus on how the stimulating paradigms can improve auditory perception. However, a look at SGN neurophysiological data show that there are definite temporal operating limits which should be considered for CI stimulation. Going forward, approaches that are successful at taking into account the temporal characteristics of the stimulus-response phenomena (or the underlying SGN neurophysiology that gives rise to them) may provide the insights necessary for significantly improving the functionality of cochlear prostheses.

ACKNOWLEDGMENTS

We would like to thank Drs. Paul Abbas, Lianne Cartee, and Elisabeth Glowatzki for allowing the use of their figures in this paper. We would also like to thank members of the Bruce laboratory for the feedback on earlier versions of the manuscript. Finally, we would like to thank Associate Editor Dr. George Spirou and the two anonymous reviewers for the helpful comments. This work was supported by NSERC Discovery Grant 261736 (ICB).

*Compliance with Ethical Standards**Conflict of Interest*

The authors declare that they have no competing interests.

REFERENCES

- ADAMSON CL, REID MA, MO ZL, BOWNE-ENGLISH J, DAVIS RL (2002) Firing features and potassium channel content of murine spiral ganglion neurons vary with cochlear location. *J Comp Neurol* 447(4):331–350
- ARORA K, DAWSON P, DOWELL R, VANDALI A (2009) Electrical stimulation rate effects on speech perception in cochlear implants. *Int J Audiol* 48(8):561–567
- AVISSAR M, WITTIG JH, SAUNDERS JC, PARSONS TD (2013) Refractoriness enhances temporal coding by auditory nerve fibers. *J Neurosci* 33(18):7681–7690
- BALKANY T, HODGES A, MENAPACE C, HAZARD L, DRISCOLL C, GANTZ B, KELSALL D, LUXFORD W, McMENOMY S, NEELY JG, PETERS B, PILLSBURY H, ROBERSON J, SCHRAMM D, TELIAN S, WALTZMAN S, WESTERBERG B, PAYNE S (2007) Nucleus Freedom North American clinical trial. *Otolaryngol Head Neck Surg* 136(5):757–762
- BAYLOR DA, NICHOLLS JG (1969) Changes in extracellular potassium concentration produced by neuronal activity in the central nervous system of the leech. *J Physiol* 203(3):555–569
- BENARROCH EE (2013) HCN channels: function and clinical implications. *Neurology* 80(3):304–310
- BENDA J, HERZ AVM (2003) A universal model for spike-frequency adaptation. *Neural Comput* 15(11):2523–2564
- BI Q (1989) A closed-form solution for removing the dead time effects from the poststimulus time histograms. *J Acoust Soc Am* 85(6):2504
- BIEL M, WAHL-SCHOTT C, MICHALAKIS S, ZONG X (2009) Hyperpolarization-activated cation channels: from genes to function. *Physiol Rev* 89(3):847–885
- BORTONE DS, MITCHELL K, MANIS PB (2006) Developmental time course of potassium channel expression in the rat cochlear nucleus. *Hear Res* 211(1-2):114–125
- BOTROS A, PSARROS C (2010) Neural response telemetry reconsidered: II. The influence of neural population on the ECAP recovery function and refractoriness. *Ear Hear* 31(3):380–391
- BRETTE R, GERSTNER W (2005) Adaptive exponential integrate-and-fire model as an effective description of neuronal activity. *J Neurophysiol* 94(5):3637–3642
- BREW HM, HALLOWS JL, TEMPEL BL (2003) Hyperexcitability and reduced low threshold potassium currents in auditory neurons of mice lacking the channel subunit Kv1.1. *J Physiol* 548(1):1–20
- BROWN DA, ADAMS PR (1980) Muscarinic suppression of a novel voltage-sensitive K⁺ current in a vertebrate neuron. *Nature* 283(5748):673–676
- BRUCE IC, WHITE MW, IRLICHT LS, O'LEARY SJ, DYNES S, JAVEL E, CLARK GM (1999) A stochastic model of the electrically stimulated auditory nerve: single-pulse response. *IEEE Trans Biomed Eng* 46(6):617–629
- BRUNEL N, VAN ROSSUM M (2007) Quantitative investigations of electrical nerve excitation treated as polarization. *Biol Cybern* 97(5-6):341–349
- BURKITT AN (2006) A review of the integrate-and-fire neuron model: I. Homogeneous synaptic input. *Biol Cybern* 95(1):1–19
- BUTIKOFER R, LAWRENCE PD (1979) Electrocutaneous nerve stimulation-II: stimulus waveform selection. *IEEE Trans Biomed Eng* BME-26(2):69–75
- CAMPBELL LJ, SLY DJ, O'LEARY SJ (2012) Prediction and control of neural responses to pulsatile electrical stimulation. *J Neural Eng* 9(2):026,023
- CARTEE LA (2000) Evaluation of a model of the cochlear neural membrane. II: Comparison of model and physiological measures of membrane properties measured in response to intrameatal electrical stimulation. *Hear Res* 146(1-2):153–166
- CARTEE LA (2006) Spiral ganglion cell site of excitation II: numerical model analysis. *Hear Res* 215(1-2):22–30
- CARTEE LA, VAN DEN HONERT C, FINLEY CC, MILLER RL (2000) Evaluation of a model of the cochlear neural membrane. I. Physiological measurement of membrane characteristics in response to intrameatal electrical stimulation. *Hear Res* 146(1-2):143–152
- CARTEE LA, MILLER CA, VAN DEN HONERT C (2006) Spiral ganglion cell site of excitation I: comparison of scala tympani and intrameatal electrode responses. *Hear Res* 215(1-2):10–21
- CHEN C (1997) Hyperpolarization-activated current (I_h) in primary auditory neurons. *Hear Res* 110(1-2):179–190
- CHOW CC, WHITE JA (1996) Spontaneous action potentials due to channel fluctuations. *Biophys J* 71(6):3013–3021
- COHEN LT (2009) Practical model description of peripheral neural excitation in cochlear implant recipients: 5. Refractory recovery and facilitation. *Hear Res* 248(1-2):1–14
- DYNES SBC (1996) Discharge characteristics of auditory nerve fibers for pulsatile electrical stimuli. PhD thesis, Massachusetts Institute of Technology, Cambridge, Massachusetts
- FLEIDERVISH IA, FRIEDMAN A, GUTNICK MJ (1996) Slow inactivation of Na⁺ current and slow cumulative spike adaptation in mouse and guinea-pig neocortical neurones in slices. *J Physiol Lond* 493(1):83–97
- FRANKENHAUSER B, VALLBO AB (1965) Accommodation in myelinated nerve fibres of *Xenopus laevis* as computed on the basis of voltage clamp data. *Acta Physiol Scand* 63(1-2):1–20
- FRIESEN LM, SHANNON RV, CRUZ RJ (2005) Effects of stimulation rate on speech recognition with cochlear implants. *Audiol Neurootol* 10(3):169–184
- GLOWATZKI E, FUCHS PA (2002) Transmitter release at the hair cell ribbon synapse. *Nat Neurosci* 5(2):147–154
- GOLDWYN JH, RUBINSTEIN JT, SHEA-BROWN E (2012) A point process framework for modeling electrical stimulation of the auditory nerve. *J Neurophysiol* 108(5):1430–1452
- GULLEDGE AT, DASARI S, ONOUE K, STEPHENS EK, HASSE JM, AVESAR D (2013) A sodium-pump-mediated afterhyperpolarization in pyramidal neurons. *J Neurosci* 33(32):13,025–13,041
- HARDIE NA, SHEPHERD RK (1999) Sensorineural hearing loss during development: morphological and physiological response of the cochlea and auditory brainstem. *Hear Res* 128(1-2):147–165
- HARTMANN R, TOPP G, KLINKE R (1984) Discharge patterns of cat primary auditory fibers with electrical-stimulation of the cochlea. *Hear Res* 13(1):47–62
- HEFFER LF (2010) High rate electrical stimulation of the auditory nerve: examining the effects of sensorineural hearing loss. PhD thesis, The University of Melbourne, Melbourne, Victoria
- HEFFER LF, SLY DJ, FALLON JB, WHITE MW, SHEPHERD RK, O'LEARY SJ (2010) Examining the auditory nerve fiber response to high rate cochlear implant stimulation: chronic sensorineural hearing loss and facilitation. *J Neurophysiol* 104(6):3124–3135
- HEIL P, NEUBAUER H, IRVINE DRF, BROWN M (2007) Spontaneous activity of auditory-nerve fibers: insights into stochastic processes at ribbon synapses. *J Neurosci* 27(31):8457–8474
- HILL AV (1936) Excitation and accommodation in nerve. *Proc R Soc B* 119(814):305–355

- HODGKIN AL (1938) The subthreshold potentials in a crustacean nerve fibre. *Proc R Soc B* 126(842):87–121
- HODGKIN AL, HUXLEY AF (1952) A quantitative description of membrane current and its application to conduction and excitation in nerve. *J Physiol* 117(4):500–544
- HOLDEN LK, SKINNER MW, HOLDEN TA, DEMOREST ME (2002) Effects of stimulation rate with the Nucleus 24 ACE speech coding strategy. *Ear Hear* 23(5):463–476
- VAN DEN HONERT C, KELSALL DC (2007) Focused intracochlear electric stimulation with phased array channels. *J Acoust Soc Am* 121(6):3703–3716
- HOSSAIN WA, ANTIC SD, YANG Y, RASBAND MN, MOREST DK (2005) Where is the spike generator of the cochlear nerve? Voltage-gated sodium channels in the mouse cochlea. *J Neurosci* 25(29):6857–6868
- HOWELLS J, TREVILLION L, BOSTOCK H, BURKE D (2012) The voltage dependence of $I(I_h)$ in human myelinated axons. *J Physiol Lond* 590(Pt 7):1625–1640
- IMENNOV NS, RUBINSTEIN JT (2009) Stochastic population model for electrical stimulation of the auditory nerve. *IEEE Trans Biomed Eng* 56(10):2493–2501
- IZHIKOVICH EM (2003) Simple model of spiking neurons. *IEEE Trans Neural Netw* 14(6):1569–1572
- JAVEL E, VIEMEISTER NF (2000) Stochastic properties of cat auditory nerve responses to electric and acoustic stimuli and application to intensity discrimination. *J Acoust Soc Am* 107(2):908
- JUNE L, YOUNG ED (1993) Discharge-rate dependence of refractory behavior of cat auditory-nerve fibers. *Hear Res* 69(1-2):151–162
- KANDEL ER, SCHWARTZ J, JESSELL T (2000) Principles of neural science, 4th edn. McGraw-Hill Medical
- KATZ B (1936) Multiple response to constant current in frog's medullated nerve. *J Physiol* 88(2):239–255
- KIEFER J, VON ILBERG C, RUPPRECHT V, HUBNER-EGNER J, KNECHT R (2000) Optimized speech understanding with the continuous interleaved sampling speech coding strategy in patients with cochlear implants: effect of variations in stimulation rate and number of channels. *Ann Otol Rhinol Laryngol* 109(11):1009–1020
- KNIGHT BW (1972) Dynamics of encoding in a population of neurons. *J Gen Physiol* 59(6):734–766
- LAI HC, JAN LY (2006) The distribution and targeting of neuronal voltage-gated ion channels. *Nat Rev Neurosci* 7(7):548–562
- LAPIQUE L (1907) Recherches quantitatives sur l'excitation électrique des nerfs traitée comme une polarisation. *J Physiol Pathol Gen* 9:620–635
- LITVAK LM, DELGUTTE B, EDDINGTON DK (2001) Auditory nerve fiber responses to electric stimulation: modulated and unmodulated pulse trains. *J Acoust Soc Am* 110(1):368–379
- LITVAK LM, SMITH ZM, DELGUTTE B, EDDINGTON DK (2003) Desynchronization of electrically evoked auditory-nerve activity by high-frequency pulse trains of long duration. *J Acoust Soc Am* 114(4 Pt 1):2066–2078
- LIU Q, LEE E, DAVIS RL (2014A) Heterogeneous intrinsic excitability of murine spiral ganglion neurons is determined by Kv1 and HCN channels. *Neuroscience* 257:96–110
- LIU Q, MANIS PB, DAVIS RL (2014B) I_h and HCN channels in murine spiral ganglion neurons: tonotopic variation, local heterogeneity, and kinetic model. *J Assoc Res Otolaryngol* 15(4):585–599
- LOIZOU PC (1998) Mimicking the human ear. *IEEE Signal Process Mag* 15(5):101–130
- LOIZOU PC, POROY O, DORMAN M (2000) The effect of parametric variations of cochlear implant processors on speech understanding. *J Acoust Soc Am* 108(2):790–802
- LUCAS K (1910) Quantitative researches on the summation of inadequate stimuli in muscle and nerve, with observations on the time-factor in electric excitation. *J Physiol* 39(6):461–475
- MACHERY O, CARLYON RP, VAN WIERINGEN A, DEEKS JM, WOUTERS J (2008) Higher sensitivity of human auditory nerve fibers to positive electrical currents. *J Assoc Res Otolaryngol* 9(2):241–251
- MADISON DV, NICOLL RA (1984) Control of the repetitive discharge of rat CA 1 pyramidal neurones in vitro. *J Physiol* 354:319–331
- MARK KE, MILLER MI (1992) Bayesian model selection and minimum description length estimation of auditory-nerve discharge rates. *J Acoust Soc Am* 91(2):989–1002
- MATSUOKA AJ, RUBINSTEIN JT, ABBAS PJ, MILLER CA (2001) The effects of interpulse interval on stochastic properties of electrical stimulation: models and measurements. *IEEE Trans Biomed Eng* 48(4):416–424
- MERZENICH MM, WHITE MW (1977) Cochlear implants: the interface problem. In: Hambrecht FT, Reswick JB (eds) *Functional electrical stimulation: applications in neural prostheses*. Marcel Dekker, Inc., New York, pp 321–340
- MILLER C, ABBAS PJ, NOURSKI KV, HU N, ROBINSON BK (2003) Electrode configuration influences action potential initiation site and ensemble stochastic response properties. *Hear Res* 175(1-2):200–214
- MILLER CA, ABBAS PJ, ROBINSON B (2001) Response properties of the refractory auditory nerve fiber. *J Assoc Res Otolaryngol* 2(3):216–232
- MILLER CA, WOO J, ABBAS PJ, HU N, ROBINSON BK (2011) Neural masking by sub-threshold electric stimuli: animal and computer model results. *J Assoc Res Otolaryngol* 12(2):219–232
- MILLER MI (1985) Algorithms for removing recovery-related distortion from auditory-nerve discharge patterns. *J Acoust Soc Am* 77(4):1452–1464
- MILLER MI, MARK KE (1992) A statistical study of cochlear nerve discharge patterns in response to complex speech stimuli. *J Acoust Soc Am* 92(1):202–209
- MINO H, RUBINSTEIN JT, MILLER CA, ABBAS PJ (2004) Effects of electrode-to-fiber distance on temporal neural response with electrical stimulation. *IEEE Trans Biomed Eng* 51(1):13–20
- MO ZL, ADAMSON CL, DAVIS RL (2002) Dendrotoxin-sensitive K⁺ currents contribute to accommodation in murine spiral ganglion neurons. *J Physiol* 542(3):763–778
- NEGM MH, BRUCE IC (2008) Effects of and on the response of the auditory nerve to electrical stimulation in a stochastic Hodgkin-Huxley model. *Proc 30th Annu Int Conf IEEE Eng Med Biol Soc* pp 5539–5542
- NEGM MH, BRUCE IC (2014) The effects of HCN and KLT ion channels on adaptation and refractoriness in a stochastic auditory nerve model. *IEEE Trans Biomed Eng* 61(11):2749–2759
- NERNST W (1908) Zur theorie des elektrischen reizes. *Pfluger Arch* 122(7-9):275–314
- NIE K, BARCO A, ZENG FG (2006) Spectral and temporal cues in cochlear implant speech perception. *Ear Hear* 27(2):208–217
- PHAN TT, WHITE MW, FINLEY CC, CARTEE LA (1994) Neural membrane model responses to sinusoidal electrical stimuli. In: Hochmair-Desoyer IJ, Hochmair ES (eds) *Advances in cochlear implants*. Manz, Vienna, Austria, pp 342–347
- PLANT K, HOLDEN L, SKINNER M, ARCAROLI J, WHITFORD L, LAW MA, NEL E (2007) Clinical evaluation of higher stimulation rates in the nucleus research platform 8 system. *Ear Hear* 28(3):381–393
- PLANT KL, WHITFORD LA, PSARROS CE, VANDALI AE (2002) Parameter selection and programming recommendations for the ACE and CIS speech-processing strategies in the Nucleus 24 cochlear implant system. *Cochlear Implants Int* 3(2):104–125
- PLOURDE E, DELGUTTE B, BROWN EN (2011) A point process model for auditory neurons considering both their intrinsic dynamics and the spectrotemporal properties of an extrinsic signal. *IEEE Trans Biomed Eng* 58(6):1507–1510

- PRIJS VF, KEIJZER J, VERSNEL H, SCHOONHOVEN R (1993) Recovery characteristics of auditory nerve fibres in the normal and noise-damaged guinea pig cochlea. *Hear Res* 71(1-2):190–201
- RASBAND MN, SHRAGER P (2000) Ion channel sequestration in central nervous system axons. *J Physiol* 525(Pt 1):63–73
- RATTAY F (2000) Basics of hearing theory and noise in cochlear implants. *Chaos Soliton Fract* 11(12):1875–1884
- RATTAY F, DANNER SM (2014) Peak I of the human auditory brainstem response results from the somatic regions of type I spiral ganglion cells: evidence from computer modeling. *Hear Res* 315:67–79
- RATTAY F, LUTTER P, FELIX H (2001) A model of the electrically excited human cochlear neuron. *Hear Res* 153(1-2):43–63
- RATTAY F, POTRUSIL T, WENGER C, WISE AK, GLUECKERT R, SCHROTT-FISCHER A (2013) Impact of morphometry, myelination and synaptic current strength on spike conduction in human and cat spiral ganglion neurons. *PLoS One* 8(11):e79,256
- REID MA, FLORES-OTERO J, DAVIS RL (2004) Firing patterns of type II spiral ganglion neurons in vitro. *J Neurosci* 24(3):733–742
- ROBINSON RB, SIEGELBAUM SA (2003) Hyperpolarization-activated cation currents: from molecules to physiological function. *Annu Rev Physiol* 65:453–480
- ROTHMAN JS, MANIS PB (2003) Kinetic analyses of three distinct potassium conductances in ventral cochlear nucleus neurons. *J Neurophysiol* 89(6):3083–3096
- RUBINSTEIN JT (1995) Threshold fluctuations in an N sodium channel model of the node of Ranvier. *Biophys J* 68(3):779–785
- SAFIEDDINE S, EL-AMRAOUI A, PETIT C (2012) The auditory hair cell ribbon synapse: from assembly to function. *Annu Rev Neurosci* 35(1):509–528
- SIGWORTH FJ (1981) Covariance of nonstationary sodium current fluctuations at the node of Ranvier. *Biophys J* 34(1):111–133
- SLY DJ, HEFFER LF, WHITE MW, SHEPHERD RK, BIRCH MGJ, MINTER RL, NELSON NE, WISE AK, O'LEARY SJ (2007) Deafness alters auditory nerve fibre responses to cochlear implant stimulation. *Eur J Neurosci* 26(2):510–522
- SMIT JE, HANEKOM T, HANEKOM JJ (2008) Predicting action potential characteristics of human auditory nerve fibres through modification of the Hodgkin-Huxley equations. *S Afr J Sc* 104(7-8):284–292
- SMIT JE, HANEKOM T, VAN WIERINGEN A, WOUTERS J, HANEKOM JJ (2010) Threshold predictions of different pulse shapes using a human auditory nerve fibre model containing persistent sodium and slow potassium currents. *Hear Res* 269(1-2):12–22
- SOLANDT DY (1936) The measurement of “accommodation” in nerve. *Proc R Soc B* 119(814):355–379
- TAIT J (1910) The relation between refractory phase and electrical change. *Exp Physiol* 3(3):221–232
- TREVINO A, COLEMAN TP, ALLEN J (2010) A dynamical point process model of auditory nerve spiking in response to complex sounds. *J Comput Neurosci* 29(1-2):193–201
- VANDALI AE, WHITFORD LA, PLANT KL, CLARKE GM (2000) Speech perception as a function of electrical stimulation rate: using the nucleus 24 cochlear implant system. *Ear Hear* 21(6):608–624
- VERSCHEUR CA (2005) Effect of stimulation rate on speech perception in adult users of the Med-El CIS speech processing strategy. *Int J Audiol* 44(1):58–63
- VERVEEN AA (1961) Fluctuation in excitability. PhD thesis, Netherlands Central Institute for Brain Research, Amsterdam, Netherlands
- VERVEEN AA (1962) Axon diameter and fluctuation in excitability. *Acta Morphol Neerl Scand* 5:79–85
- VERVEEN AA, DERKSEN HE (1968) Fluctuation phenomena in nerve membrane. *Proc IEEE* 56(6):906–916
- WEBER BP, LAI WK, DILLIER N, VON WALLENBERG EL, KILLIAN MJP, PESCH J, BATTMER RD, LENARZ T (2007) Performance and preference for ACE stimulation rates obtained with nucleus RP 8 and freedom system. *Ear Hear* 28(2):46S–48S
- WEBSTER M, WEBSTER DB (1981) Spiral ganglion neuron loss following organ of Corti loss: a quantitative study. *Brain Res* 212(1):17–30
- WHITE MW (1984) Psychophysical and neuropsychological considerations in the design of a cochlear prosthesis. *Audiol Ital* 1:77–117
- WILSON BS, FINLEY CC, FARMER JC, LAWSON DT, WEBER BA, WOLFORD RD, KENAN PD, WHITE MW, MERZENICH MM, SCHINDLER RA (1988) Comparative studies of speech processing strategies for cochlear implants. *Laryngoscope* 98(10):1069–1077
- WILSON BS, FINLEY CC, LAWSON DT, WOLFORD RD, ZERBI M (1993) Design and evaluation of a continuous interleaved sampling (CIS) processing strategy for multichannel cochlear implants. *J Rehabil Res Dev* 30(1):110–116
- WOO J, MILLER CA, ABBAS PJ (2009A) Biophysical model of an auditory nerve fiber with a novel adaptation component. *IEEE Trans Biomed Eng* 56(9):2177–2180
- WOO J, MILLER CA, ABBAS PJ (2009B) Simulation of the electrically stimulated cochlear neuron: modeling adaptation to trains of electric pulses. *IEEE Trans Biomed Eng* 56(5):1348–1359
- WOO J, MILLER CA, ABBAS PJ (2009C) The dependence of auditory nerve rate adaptation on electric stimulus parameters, electrode position, and fiber diameter: a computer model study. *J Assoc Res Otolaryngol* 11(2):283–296
- YI E, ROUX I, GLOWATZKI E (2010) Dendritic HCN channels shape excitatory postsynaptic potentials at the inner hair cell afferent synapse in the mammalian cochlea. *J Neurophysiol* 103(5):2532–2543
- ZHANG F, MILLER CA, ROBINSON BK, ABBAS PJ, HU N (2007) Changes across time in spike rate and spike amplitude of auditory nerve fibers stimulated by electric pulse trains. *J Assoc Res Otolaryngol* 8(3):356–372